Structure, Vol. 11, 435–443, April, 2003, ©2003 Elsevier Science Ltd. All rights reserved. DOI 10.1016/S0969-2126(03)00044-3

Solution Structure of MT_nc, a Novel Metallothionein from the Antarctic Fish *Notothenia coriiceps*

Clemente Capasso,[1] Vincenzo Carginale,[1] Orlando Crescenzi,[2] Daniela Di Maro,[3] Elio Parisi,[1] Roberta Spadaccini,[2] and Piero Andrea Temussi[2,4,*]

[1]CNR
Institute of Protein Biochemistry
via Marconi 10
I 80125 Naples
Italy

[2]Department of Chemistry
University of Naples "Federico II"
via Cinthia 45
I 80126 Naples
Italy

[3]BIOMODEM pscrl
via Fiorentina
I 53100 Siena
Italy

[4]National Institute for Medical Research
Medical Research Council
The Ridgeway
Mill Hill
London NW7 1AA
United Kingdom

Summary

The structure of [$^{113}Cd_7$]-metallothionein (MT_nc) of the Antarctic fish *Notothenia coriiceps*, the first three-dimensional structure of a fish metallothionein, was determined by homonuclear ^1H NMR experiments and heteronuclear [^1H, ^{113}Cd]-correlation spectroscopy. MT_nc is composed of an N-terminal β domain with 9 cysteines and 3 metal ions and a carboxy-terminal α-domain with 11 cysteines and 4 metal ions. The position of the ninth Cys of the α domain of MT_nc is different from the corresponding Cys of mammalian MTs. As a result, the last CXCC motif in the mammalian MT sequence becomes CXXXCC in the fish MT. This difference leads to a structural change of the α domain and, in turn, to a different charge distribution with respect to that observed in mammalian metallothioneins.

Introduction

Among all known proteins, metallothioneins (MTs) have the most striking peculiarities. They are small in size (typically 6–7 kDa), rich in cysteines (20 residues per protein molecule), and lack well-defined secondary structure elements. Indeed, their fold is dictated mostly by a clustered network of metal-thiolate bonds among the sulfur atoms of the cysteine residues and the metal ions, usually represented by zinc, copper, and cadmium [1]. The role played by MTs has been debated for a long time, but the high thermodynamic and low kinetic stability suggest that they may bind the metal moiety with a considerable stability, providing at the same time a facile metal exchange with other proteins. Because of the unusual capability to sequester heavy metals, MTs may also act as a defense against the harmful effects of toxic elements, primarily cadmium and mercury [2].

A great deal of knowledge on the chemical features of MTs has arisen from the determination of three-dimensional structures obtained mainly by NMR spectroscopy [3–9], but also by X-ray crystallography [10, 11]. The results reported insofar demonstrate that the 3D solution structures of mammalian MTs are very similar, featuring identical cluster topology and polypeptide folding. The three-dimensional structure of the sea urchin MT has a cluster topology similar to that of evolutionary distant MTs but displays some differences in both backbone folding and connectivity pattern of the sulfur-metal bonds [8]. A comparative study of the chemical features of vertebrate MTs may contribute to a better understanding of the biological functions of MTs. Such a study has never been performed because, among vertebrates, the only MT structures available are those of mammalian origin. At first glance, the striking similarity of MT sequences from different classes of vertebrates suggests the existence of an almost equal likeness at the structural level. Indeed, all vertebrate MTs display the same arrangement of the cysteine-containing motifs, with the exception of fish MTs, in which the last CXCC motif in the α domain becomes CXXXCC [12]. Such a synapomorphism may have important structural and, possibly, functional consequences in fish MTs.

In previous papers, we have studied piscine MTs and, in particular, compared the physicochemical characteristics of the MT of *Notothenia coriiceps*, an Antarctic fish, with those of the mouse MT [12–15]. The two proteins differ markedly in the amino acid residues placed between the cysteines and, consequently, in the value of the hydrophobicity index. A preliminary study carried out on a fish MT with the use of NMR spectroscopy unveiled a selective broadening of the heteronuclear spectra that may reflect a higher structural flexibility [15]. Two-dimensional [^1H, ^{113}Cd]-correlation experiments of *N. coriiceps* MT_nc show a difference in intensity of the [^1H, ^{113}Cd] correlations between the α and β domains that is apparently higher than in the corresponding spectra of mammalian MTs.

The fact that the observed broadening does not affect the homonuclear spectra suggests an exchange phenomenon involving the metal ions that is much more pronounced in fish MT than in mouse MT. NMR observations are paralleled by both circular dichroism and dynamic fluorescence spectra of fish MT that are considerably influenced by temperature, whereas the mouse MT is much less affected by heating. An additional distinct feature of fish MT is the more pronounced reactivity of

*Correspondence: pat@chemistry.unina.it

Key words: Antarctic fish; electrostatic potential; ion exchange; NMR; poikilotherm organism; zinc homeostasis

the metal-thiolate clusters in the presence of the redox couple formed by reduced and oxidized glutathione [15].

In the present report, we describe the first three-dimensional structure of a fish MT. The sequential ^{1}H-NMR assignments and subsequent structure determination were performed on the recombinant *Notothenia coriiceps* Cd_7-MT_nc by homonuclear and heteronuclear NMR spectroscopy. The position of the ninth Cys of the α domain of MT_nc, as of other piscine MTs, is different from the corresponding Cys of mammalian MTs. In the new structure, this difference leads to a structural change of the α domain and, in turn, to a different charge distribution with respect to that observed in mammalian metallothioneins.

Results

Structure Determination

The NMR structure determination of *N. coriiceps* [Cd_7^{2+}]-MT_nc was performed at pH 7.0 and 293 K with natural abundance or ^{113}Cd-labeled recombinant protein samples [15]. All attempts to measure additional restraints via ^{15}N and/or ^{13}C labeling were frustrated by the negligible yields of properly folded protein expressed in minimal media. This situation is not new in the field of MTs, since all previous structural determinations have been performed only with NOEs collected in homonuclear experiments. This approach, although at variance with state of the art structure determination of larger proteins by NMR, remains acceptable for small proteins, such as the domains of MTs, whose fold is dominated by the clustered network of metal-thiolate bonds among the sulfur atoms of the cysteine residues and the metal ions.

Resonance assignments were obtained by standard procedures. COSY [16], TOCSY [17], and NOESY [18] experiments were used for spin system identification. The assignments for the backbone amide protons and the α-carbon hydrogen atoms are complete except for the two initial residues (Gly1 and Ser2) of the hexapeptide N-terminal segment added in the expression protocol. Most nonexchangeable side chain protons were assigned. Analysis of the $^3J_{HN\alpha}$ and $^3J_{\alpha\beta}$ coupling constants together with the corresponding intraresidual and sequential NOEs with the program HABAS [19] yielded stereo-specific assignments for 13 βCH_2 groups out of the 45 nondegenerate β-methylene resonances.

The distribution of the Cd^{2+} ions into two clusters of four and three metals was based on the thiolate-metal connectivities directly measured by means of 2D [^{1}H, ^{113}Cd]-COSY spectra [20]. The two globular domains of MT_nc were termed the β domain (N terminal, 9 cysteines and 3 metal ions) and α domain (C terminal, 11 cysteines and 4 metal ions), according to the convention employed for mammalian MTs (e.g., see [5]).

Interproton distances were derived from the cross-peak integrals on 2D NOESY spectra in H_2O or ^2H_2O solution with a 150 ms mixing period. The peak integrals were evaluated with the program NMRView [21], transferred to the program package DYANA 1.5 [22], and converted to a total of 1170 upper distance limits with CALIBA [23]. The $^3J_{NH\text{-}\alpha CH}$ coupling constants were measured by the methods of Kim and Prestegard [24] and Titman and Keeler [25], and the $^3J_{\alpha\beta}$ coupling constants were measured by E-COSY experiments [26]. In the structure calculation with DYANA, spin coupling values were input into HABAS to obtain the possible range of torsion angles with simultaneous consideration of the NOE-derived distance restraints, to yield a total of 103 angular constraints. Additional constraints were furnished by Cd^{2+}-sulfur bonds [3].

Since we could not detect any long-range interdomain NOEs, separate structure calculations were performed for the two domains. For the β domain, the input for the final structure calculation with the program DYANA [22] consisted of 253 NOE upper-limit distance constraints, 12 Cd-S bond constraints, and 63 dihedral angle constraints; for the α domain there were 373 NOE distance constraints, 16 Cd-S bond constraints, and 50 dihedral angle constraints, amounting to more than 14 constraints per residue. The good rmsd of the best 20 structures (0.44 for the α domain) together with the small size and number of residual constraint violations in the DYANA runs shows that the input data represent a self-consistent set and that the constraints are well satisfied in the calculated conformers. As a further refinement, we performed a restrained energy minimization on the 40 DYANA structures with the lowest target function values with the SANDER module of the AMBER 5.0 package [27]. The best 20 structures were selected to represent the solution structure. The quality of the structure determination is reflected by global rmsd values relative to the mean coordinates for the backbone atoms of both domains (Table 1). The core of the α domain is characterized with greatest precision; the rmsd calculated for the backbone heavy atoms of residues 31–59 is 0.44 Å (Table 1). Figure 1 shows the bundle of the best 20 structures for the two domains separately, since we did not detect any interdomain NOEs. The total lack of correlation between the two domains, although common to all other solution studies, is at variance with the correlation found in the crystal structure of rat liver MT2 [10], where correlation may be induced by crystallization [28].

However, the observation that the two domains do not interact in any significant way relies on the possibility of detecting a number of weak NOEs between pairs of protons belonging to different domains. Such effects, if present, may be so weak as to be virtually undetectable among the stronger intraresidue NOEs in crowded 2D spectra. On the other hand, it can be predicted that even minor interactions between the two domains can affect the chemical shifts of protons of either domain, since the dependence of chemical shifts even on small local environmental changes is highly nonlinear. It is common experience in NMR spectroscopy of proteins that large differences in chemical shifts can occur as a consequence of minor structural differences, whereas the opposite, i.e., small differences in chemical shifts between substantially different structures, is virtually impossible. Accordingly, we have compared the spectra of the isolated domains with the corresponding spectra of the same domain in the whole protein (data not shown). The superposition of partial NOESY spectra of the isolated α domain and of the whole metallothionein showed conclusively that corresponding resonances occupy virtually the same position, a clear proof of complete lack of correlation between the α and the β domains of MT_nc.

Table 1. Summary of Restraints and Structural Statistics

	α Domain (31–60)	β Domain (4–30)
Restraints		
NOEs		
Intraresidue	159	137
Sequential	123	94
Medium-range (i < 5)	60	20
Long-range	31	2
Total NOEs	373	253
Dihedral angles	50	63
Precision[a]		
Backbone heavy atoms (Å)	0.44 ± 0.7	1.61 ± 0.06
All heavy atoms (Å)	0.71 ± 0.15	2.03 ± 0.12
S^{γ} and Cd atoms (Å)	0.21 ± 0.1	0.33 ± 0.1

[a] Average coordinates of the 20 energy-minimized conformers after superposition for the best fit of the atoms of the residues indicated in parentheses.

The NMR Solution Structure of *Notothenia coriiceps* [Cd_7^{2+}]-MT

The three-dimensional structure of *N. coriiceps* [Cd_7^{2+}]-MT_nc is characterized by the presence of two domains linked by Lys29-Lys30, i.e., a C-terminal α domain comprising residues 31–60 and a four-metal cluster and an N-terminal β domain comprising residues 1–28 and a three-metal cluster.

The following secondary structure elements can be identified. One α helical region from Thr41 to Ala44 and one 3_{10} helix from Val48 to Lys50 are clearly identifiable in nearly all structures of the bundle of the α domain, whereas only one α-helical stretch from Glu5 to Ser9 could be identified in most structures of the β domains.

The lower average number of NOEs per residue in the β domain of MT_nc results in a lower precision of the structure determination for the backbone when compared to the α domain (Table 1). The architecture of both domains is determined by the Cd-Cys clusters, as is the case for all metallothioneins. MT_nc, however, like other MTs from teleosts, has a significant sequence difference involving Cys54 that is not aligned with the corresponding Cys of mammalian MTs. This difference has important consequences on the structure of the α domain. Figure 2 shows the alignment of the sequence of MT_nc with those of a few representative mammalian metallothioneins along with the 3D alignment of the structures of the α domains of MT_nc and mouse MT-I obtained by fitting all Cys residues, except Cys54 of MT_nc and Cys56 of MT-I.

The main consequence of the displacement of "anomalous" Cys54 with respect to the corresponding Cys of mouse MT is the induction of a drastically different orientation of the loop Lys50-Gly51-Lys52-Thr53 of MT_nc with respect to the corresponding Lys52-Gly53-Ala54-Ala55 loop of mouse MT-I. Figure 2A shows the superposition of the neon representations of models of the α domains of fish (MT_nc; magenta) and mammal (mouse MT-I; green). It is easy to see that, in MT_nc, the loop rotates down, opening a wide channel. For better visualization of this channel, Figure 2B shows another model of the α domain of MT_nc, with backbone heavy atoms represented by magenta balls with their van der Waals radium.

The different alignment of the loops is paralleled by a notably different arrangement of charged residues on the surface. The sequence of the α domain of *Notothenia* has the same number of basic and acidic residues as

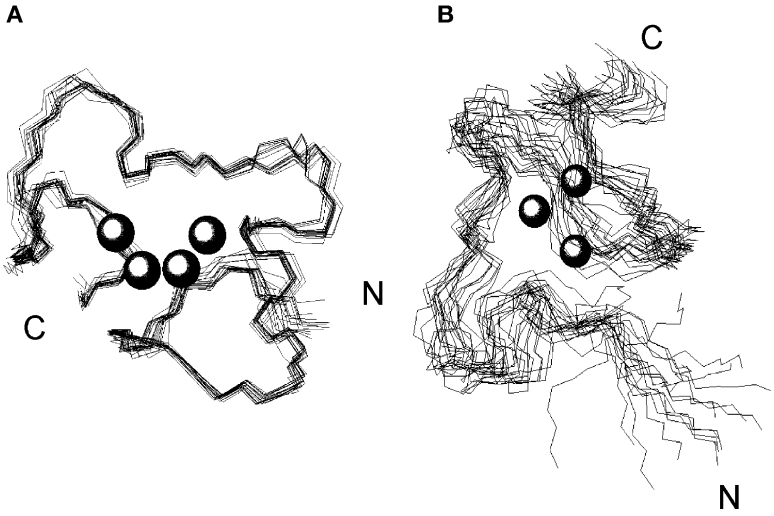

Figure 1. NMR Solution Structure of MT_nc

(A) Superposition of the backbone heavy atoms (N, C^{α}, and C′) of residues 31–60 of the 20-best energy-minimized structures (α domain). The termini are indicated by N and C labels.

(B) Superposition of the backbone heavy atoms (N, C^{α}, and C′) of residues 2–28 of the 20-best energy-minimized structures (β domain). The Cd ions are shown as balls. The termini are indicated by N and C labels. The models were generated with MOLMOL [41].

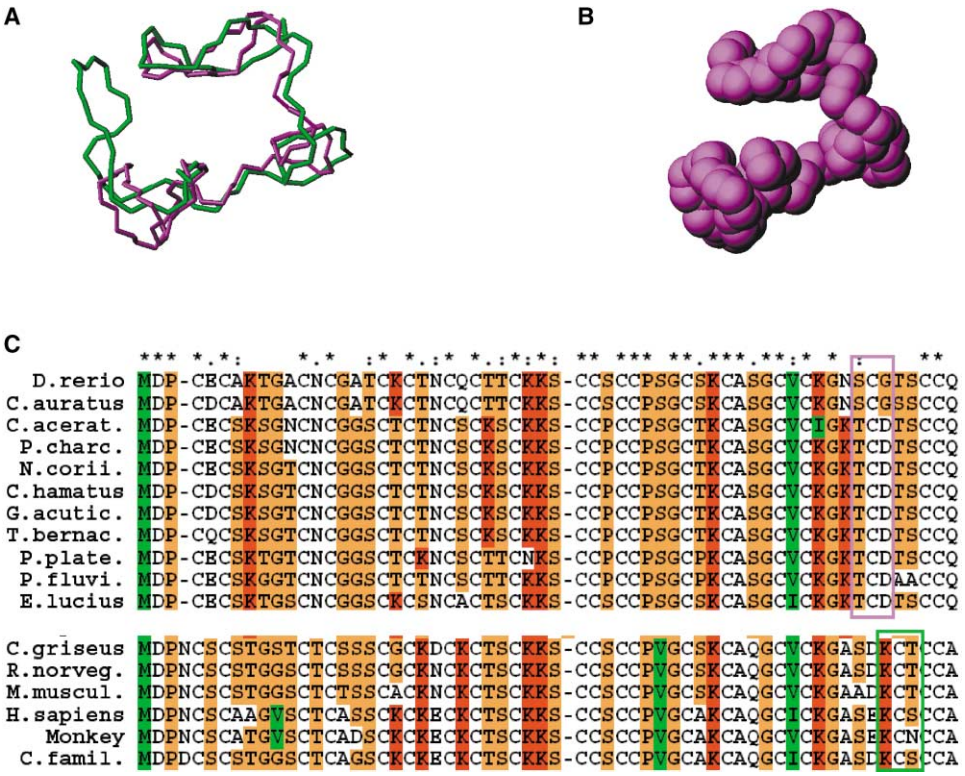

Figure 2. Alignments of Fish and Mammal MTs

(A) Superposition of the neon representations of models of the α domains of fish (MT_nc; magenta) and mammal (mouse MT-I; green).

(B) Atom representation of the α domain of MT_nc; backbone heavy atoms are represented as magenta balls with dimensions corresponding to their van der Waals radii.

(C) Sequence alignment of representative fish and mammal MTs. The regions hosting the crucial Cys residue in typical fish or mammal sequences are boxed with magenta and green linings, for fish and mammal sequences, respectively. The models were generated with MOLMOL [41]. Sequence alignment was performed with CLUSTAL X [44].

the mouse (Lys42, Lys50, Lys52, and Asp55 for the fish α domain and Lys43, Lys51, Lys56, and Asp55 for mouse α domain), but their distribution on the surface of the domain is different, mainly as a consequence of the "misalignment" of Cys54. Figure 3 shows a comparison of the surface contact plots, colored according to the electrostatic potential, of the α and β domains of fish (MT_nc) and mouse (MT-I) metallothioneins that illustrates this point. The surfaces of the α and β domains of piscine MT compared with those in mammalian MT differ both in the number and distribution of charged residues. Figure 3A shows that the charge distribution on the surface of the α domains, in spite of the fact that the charged residues are the same, is rather different between fish and mouse. Particularly, the negative charges in the fish domain are concentrated in a small area, corresponding to the mouth of the channel of Figure 2B. The different distribution in the fish β domain was expected, since it has an additional acidic residue with respect to the corresponding mouse domain: Lys8, Lys26, Asp2, and Glu5 for fish and Lys22, Lys25, and Asp2 for mouse. Nonetheless, the difference shown by Figure 3B is striking; the largely negative face of the fish domain is not present in the corresponding mouse domain.

Relationship between Structural Features and Chemical Reactivity

The distinctive structural features characterizing fish and mammalian MTs prompted us to compare the chemical reactivity of the metal-thiolate clusters of fish MT with that of the metal-thiolate clusters of mouse MT-I. In particular, we have tested the reactivity of the sulfydryl groups with Ellman's reagent [5,5′-dithiobis (2-nitrobenzoate) (DTNB)] and the Zn^{2+}/Cd^{2+} exchange. Figure 4A shows the titration of the thiol groups of the cysteine residues of fish and mouse MTs by DTNB. The results show that the number of titrated cysteines is lower in fish MT than in mouse MT. Fish MT, on the other hand, displays a better metal exchange capability with respect to mouse MT; indeed, the number of Cd^{2+} ions substituting for Zn^{2+} in $[Zn_7^{2+}]$-MT_nc is higher than in MT-I (Figure 4B). The different reactivity of fish and mouse MTs with DTNB can be attributed to the localization of the negative charge on the surface of fish MT that may hamper the interaction with this anionic reagent (see Figure 3). It is worth recalling that the net charge, as given by the algebraic sum of all charged residues, including cysteines and metal ions, is also different for the two proteins: that is, −3 for MT_nc and −1 for mouse MT-I. The Zn^{2+}/Cd^{2+} exchange, on the other hand, is

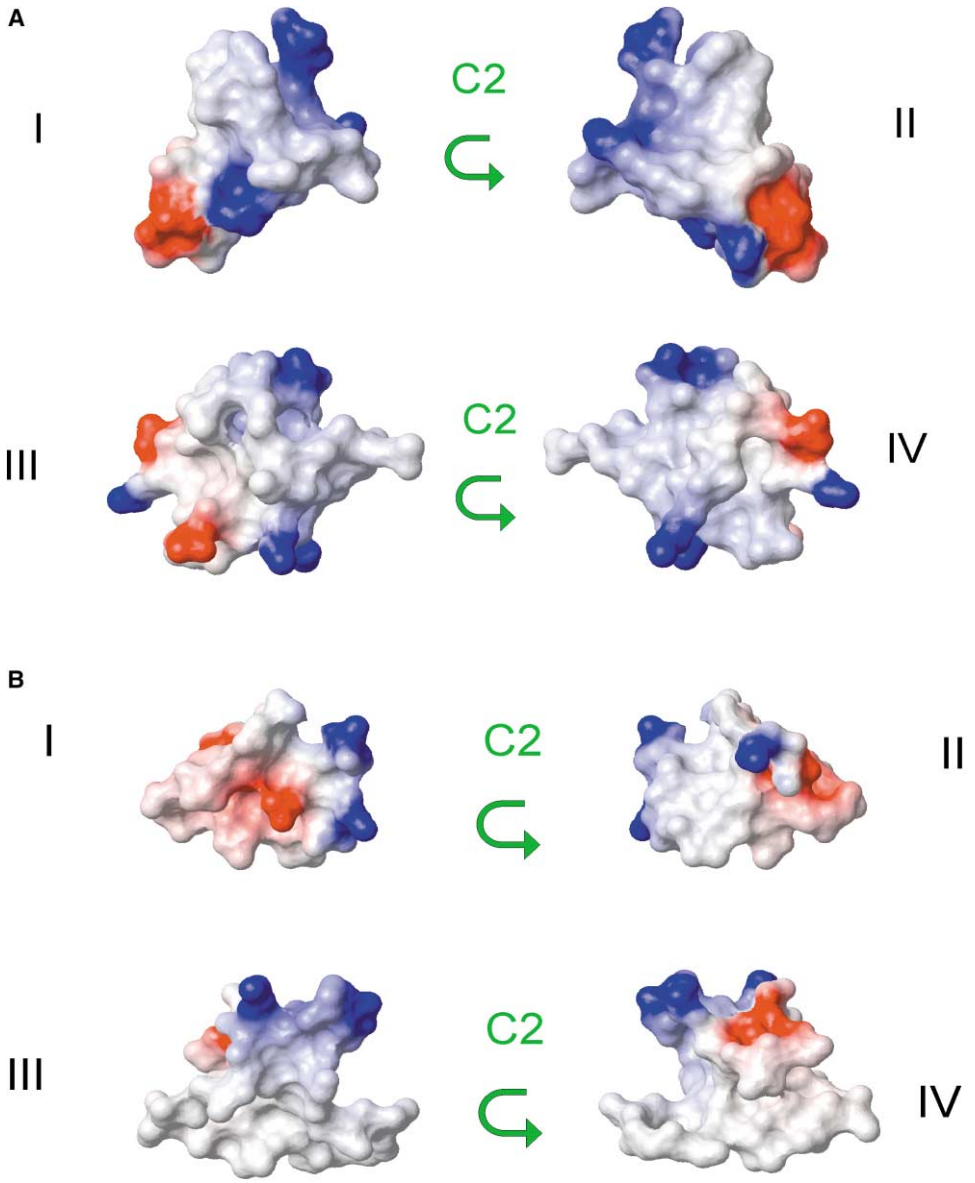

Figure 3. Surface Electrostatic Potentials of Fish and Mammal MTs

(A) Comparison of the surface contact plots of the α domains of metallothioneins of fish (MT_nc; panels I and II for two views related by a C2 axis) and mouse (MT-I; panels III and IV for the two corresponding views related by a C2 axis).

(B) Comparison of the surface contact plots of β domains of metallothioneins of fish (MT_nc; panels I and II for two views related by a C2 axis) and mouse (MT-I; panels III and IV for the two corresponding views related by a C2 axis). The surfaces are colored according to the electrostatic potential. Calculation of the electrostatic potential and generation of models were performed with MOLMOL [41].

favored by the net negative charge of fish MT that lowers the stability of the Zn^{2+}-thiolate complex. Indeed, in the case of hamster MT, it had already been shown that replacement of three lysine residues by glutamic acid affects the metal-thiolate interaction without altering the overall structure [29]. In addition, in fish MT, there is a different accessibility of the thiol groups because of conformational modifications induced by the shifted cysteine residue. The comparison of the backbone structures of fish MT with those of mouse MT-I reported in Figure 2 shows quite clearly that the main structural consequence of the Cys back shift is the opening of a wide channel on the surface of the α domain.

Discussion

The high similarity typical of vertebrate MTs allowed the grouping of these proteins in a single gene family. However, as a result of mutational events, a number of sequence-specific characters appeared during evolution, resulting in a moderate variability of the amino acid residues, other than cysteines, in MTs of different organisms. It has long been known that, among vertebrates, the amino-terminal region exhibits typical species-specific characteristics [30], conferring distinct antigenic properties to the proteins. Although the major structural constraint is represented by the arrangement

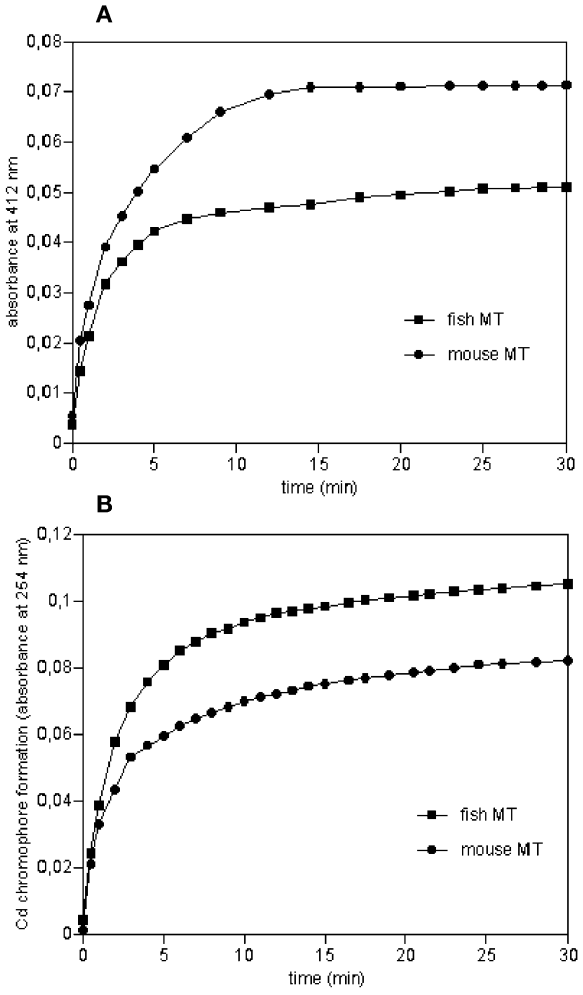

Figure 4. Comparison of the Thiol Group Accessibility and Metal Exchange of Fish and Mammal MTs

(A) Titration of reactive cysteinyl groups with DTNB. The reaction was carried out as described in Experimental Procedures.

(B) Zn^{2+}/Cd^{2+} exchange in mouse and fish Zn_7MT. The exchange reaction was followed as described in Experimental Procedures, by measuring the formation of the Cd^{2+}-thiolate chromophore.

of the 20 cysteines and by the well-defined architecture of the metal-thiolate clusters, the residues placed between the cysteine residues may affect the structure of the protein. The case of two MT isoforms found in the snail *Helix pomatia* is paradigmatic [31]. The two proteins are expressed in different tissues of the same organism by distinct genes and differ in a limited number of amino acid substitutions at positions not occupied by cysteines. In spite of such a striking similarity, one isoform binds cadmium and the other binds copper, leading to the formation of two structurally different complexes.

Piscine MTs show a number of distinctive features with respect to their mammalian counterparts, the most striking of which are the displacement of the ninth cysteine residue of the α domain and a different number of CK (or KC) motifs along the polypeptide chain. In the present paper we report the three-dimensional structure of [$^{113}Cd_7$]-metallothionein of the Antarctic fish *Notothenia coriiceps*, the first fish MT to be characterized from a structural point of view. The architecture of the two domains, as derived from the NMR analysis, resembles closely the corresponding domains of mammalian MTs [32]. The presence of the six extra amino acid residues that were added at the N terminus to express the recombinant proteins does not affect the overall shape of the protein or the essential features of the metal-thiolate clusters, as demonstrated by the fact that recombinant mouse MT-I shows the same spectroscopic properties of native rabbit MT-I [33]. However, the sequence difference involving Cys54 has important consequences on the structure of the α domain. The position of Cys54 induces a drastic difference in the orientation of the loop Lys50-Gly51-Lys52-Thr53 with respect to the corresponding Lys52-Gly53-Ala54-Ala55 of MT-I, and this difference, in turn, induces a different distribution of charges on the surface of the α domain.

Another interesting peculiarity of fish MT, with no counterpart in mouse MT, is given by the presence of an α-helical region spanning residues Thr41–Ala44 and a 3_{10} helix from Val48 to Lys50 in the α domain and by the presence of an α-helical stretch spanning Glu5–Ser9 in the β domain. The existence of short α helix elements was postulated to explain features of the FT-IR spectra of fish MT [34]. A clear transition, monitored by the position of the α helix band and corresponding to the onset of unfolding at 30°C, was registered in coincidence with changes of the metal-thiolate complex. This effect may be attributed to the presence of cysteine residues in the two α helices found in fish MT.

The results of our recent studies showed that the optical properties of fish and mouse MTs are sensitive to temperature, but in a markedly different way [15]. It was postulated that the different temperature-induced modifications of the optical properties observed in fish and mammalian MTs may be due to the lower number of (CK) motifs in fish MT. As pinpointed in earlier studies but also discussed in this paper, cysteine 54 is back shifted by two positions in piscine MT with respect to cysteine 56 of mammalian MT. As a result of such a modification, the last CXCC motif in the mammalian MT sequence becomes CXXXCC in fish MT; in light of the present structure determination, it is now possible to discuss this peculiarity in structural terms and, possibly, to link it to the kinetics of ion exchange.

In spite of the elusive role played by metallothionein, any biological function postulated for this protein turns out to be closely related to the structure of the metal-thiolate clusters and to their ability to exchange metal. Indeed, notwithstanding the apparent rigidity of the molecule, metallothionein is in a dynamically active state, with a continuous redistribution of the metal ions inside and within clusters. However, the possibility that differences in metallothionein structure could affect the cluster reactivity has not yet been explored. The most prominent difference between fish and mammalian MTs is the difference in dynamical behavior between the two domains (α and β). In fact, the [^{1}H, ^{113}Cd]-correlation NMR experiment on *N. coriiceps* MT (Figure 5) shows a difference in intensity of the [^{1}H, ^{113}Cd] correlations from the two domains that is much more pronounced

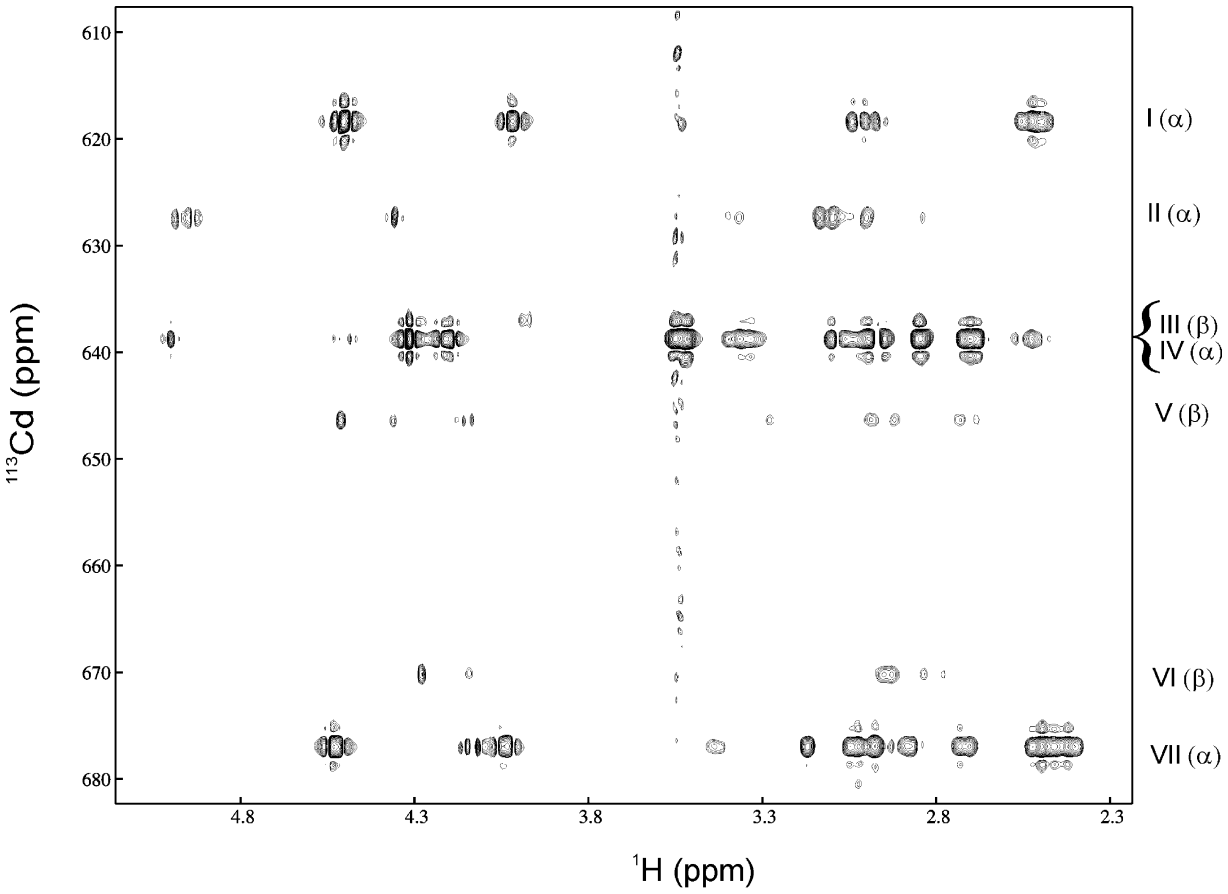

Figure 5. 2D [^{1}H, ^{113}Cd] Long-Range Correlation Spectrum of *N. coriiceps* Cd-MT

The spectrum was collected at 303 K and 400 MHz proton Larmor frequency, with an evolution time for the heteronuclear coupling of 30 ms. The Cd resonances, labeled I–VII in order of increasing chemical shift, are grouped in β and α domains.

than in mammalian MTs (e.g., see [32]). Our present results show significant differences in cysteine reactivity and metal exchangeability between fish and mouse metallothioneins, suggesting a close relationship between structural diversity and protein reactivity. Although difficult to correlate quantitatively, it is tempting to suggest that kinetic data reflect not only the conformational differences between the two proteins, but also the change of surface charge distribution from mammal to piscine MT.

Another feature of fish MT that must be taken into account is its larger hydrophilicity with respect to mammalian MT [43], a characteristic that is positively correlated to molecular flexibility. Indeed, the observed broadening of resonances, particularly evident for the β domain, may be partially attributed to the larger flexibility of MT_nc. This is in agreement with our previous studies carried out with the aid of dynamic fluorescence spectroscopy showing that MT_nc possesses a more flexible structure than mouse MT-I [34]. As proteins from cold-adapted organisms are often characterized by a higher hydrophilicity accompanied by a larger flexibility, it is possible that the structural variability observed in MTs of various origin may reflect functional and physiological differences. In this context, it is interesting that structural divergences within the MT family reflect their phylogenetic relationships [42].

Biological Implications

Metallothioneins (MTs) are low-molecular weight, cysteine-rich proteins provided with high metal binding capacity. Several biological roles have been invoked for MTs, e.g., they may be shields against toxic heavy metals (Cd, Hg, and Pb), active agents in the homeostasis of Zn^{2+} and Cu^{2+}, or scavengers of superoxide radicals in oxidative stress. A possible way to validate these hypotheses or to discriminate between them would be to establish structure-activity correlations with several MTs from different organisms. However, the available structures concern MTs of mammalian origin that are very similar, as a direct consequence of the extreme similarity of their sequences.

MTs of teleosts stand out among MTs for two peculiar features: the shift of a C-terminal Cys and a smaller number of CK (KC) motifs. It was known that they have different thermostability, different metal affinity, and different redox properties with respect to mammalian MTs, but it was not known whether they also have a different 3D structure or, most of all, whether their structure correlates with these differences. The structure of MT_nc shows indeed that, in the α domain, the unusual sequence induces a major structural change, in the form of a large displacement of a loop, and this change, in turn, leads

to a different distribution of charges on the surface. In addition, the β domain MT_nc hosts an extra charged residue (E5), leading once again to a different surface charge distribution with respect to mammalian MTs. The main biological implication of the present structural work is that the marked difference in the distribution of surface charges can have a profound influence on the kinetics of ion exchange. The propensity of MT_nc to release or exchange zinc more easily than its mammalian counterpart suggests that zinc-dependent processes may be differentially regulated in poikilotherm and homeotherm organisms. The larger flexibility of MT_nc is a feature frequently found in cold-adapted proteins.

Experimental Procedures

Sample Preparation

The recombinant polypeptide of *Notothenia coriiceps* (Antarctic fish) MT_nc was obtained and expressed in *E. coli* strain BL21 (DE3), as described in [15]. The cells were grown until mid-log phase ($O.D._{590}$ = 0.6). At this point IPTG and $CdSO_4$ ($^{113}CdSO_4$ for the labeled sample) were added to a final concentration of 0.1 mM. After incubation for a further 3 hr at 37°C, cells were pelleted by centrifugation at 6000 rpm for 20 min and washed two times in PBS (140 mM NaCl, 2.7 mM KCl, 10 mM Na_2HPO_4, and 1.8 mM KH_2PO_4 [pH 7.3]). The pelleted cells were resuspended in 5% of the original volume of PBS containing 3 mM β-mercaptoethanol and lysed by mild sonication at 4°C. Triton X-100 was added to a final concentration of 1%, and the suspension was mixed gently at room temperature for 1 hr to facilitate solubilization of proteins. The recombinant fusion protein (GST-MT) was purified by affinity chromatography with a column of glutathione Sepharose 4B (Pharmacia Biotech, Sweden) equilibrated with PBS. The supernatant was applied on an affinity column and then extensively washed with equilibration buffer. The GST-MT was eluted with 10 mM glutathione in 50 mM Tris-HCl (pH 8.0). The fusion protein containing fractions were pooled, digested with thrombin, and then fractionated on a column of Sephadex G-75 (45 × 1.5 cm) equilibrated with 0.02 M Tris-HCl buffer (pH 8.00). Column eluate was collected in 1 ml fractions and monitored for absorbance at 254 nm and cadmium contents. The peak corresponding to recombinant MT was lyophilized.

NMR Spectroscopy

Approximately 2 mM samples of recombinant *N. coriiceps* MT_nc were prepared by dissolving appropriate amounts of protein in either in 95% H_2O/5% D_2O or in D_2O at pH 7.0 under argon. Experiments were run on Bruker DRX-400 and DRX-600 spectrometers at 293 K. Data processing was performed with NMRPipe [35], and spectral analysis was performed with NMRView [21]. A conventional set of 2D spectra, COSY [16], TOCSY [17], NOESY [18], and double quantum coherence [36], was used for sequential assignment according to the scheme described by Wüthrich [37]. TOCSY spectra were collected with a mixing time of 75 ms, by the DIPSI2-rc mixing scheme [38]. NOESY spectra were recorded with mixing time of 150 ms. TPPI was applied to achieve quadrature detection in the indirect dimension [39]. Water suppression was achieved either by presaturation or by the WATERGATE pulse sequence [40]. Proton-detected [^{1}H, ^{113}Cd] heteronuclear long-range correlation spectra were collected on a ^{113}Cd-enriched sample over a range of evolution times (15–30 ms), by either gradient coherence selection or conventional phase cycling. $^3J_{NH\text{-}\alpha}$ coupling constants were estimated with the methods of Kim and Prestegard [24] and Titman and Keeler [25]; $^3J_{\alpha\text{-}\beta}$ coupling constants were measured by E-COSY experiments [26].

Collection of Constraints and Calculation of the Structure

Distance constraints were obtained from NOESY crosspeak volumes. A mixing time of 150 ms was used for both sequential assignments and partial constraint collection in a NOESY experiment recorded at 400 MHz on the protonated sample. The corresponding experiment in D_2O was recorded at 600 MHz with a mixing time of 60 ms. The metal-sulfur connectivities were derived from the [^{1}H, ^{113}Cd]-COSY data, assuming tetrahedral symmetry for the Cd ions. Distance constraints of the Cd-sulfur bonds were chosen according to Arseniev et al. [3]. $^3J_{\alpha\text{-}\beta}$ coupling constants were measured by E-COSY experiments [26], whereas $^3J_{NH\text{-}\alpha}$ coupling constants were estimated by the methods of Kim and Prestegard [24] and Titman and Keeler [25]. In the structure calculation with DYANA, spin coupling values were input into HABAS to obtain the possible range of torsion angles with simultaneous consideration of the NOE-derived distance restraints, to yield a total of 184 angular constraints [19]. A total of 1170 NOESY crosspeaks were determined and, after selection of redundancies and inconsistencies with the aid of CALIBA, in the present calculation, 734 distance and 184 dihedral angle restraints were incorporated.

Separate structure calculations were done for the β domain containing residues 1–28 and for the α domain containing residues 31–60, with the exclusion of the linker Lys29-Lys30 peptide. The final round of DYANA structure calculations was started with 40 randomized conformers. The 20 DYANA conformers with the smallest target function values were chosen to represent the three-dimensional NMR structure. All color figures were generated with the program MOLMOL [41].

Sulfydryl Reactivity of the [Zn_7^{2+}]-MT

The sulfydryl reactivity of the fish and mouse [Zn_7^{2+}]-MT was assayed spectrophotometrically at 412 nm and 25°C, with 5,5′-dithiobis(2-nitrobenzoic acid) (DTNB), by the procedure described by Jiang and coworkers [43]. The reactivity of the MTs (10 μM) with DTNB (4 μM) was measured in 0.2 M Tris-HCl (pH 7.4).

Kinetics of Zn^{2+}/Cd^{2+} Substitution

The cadmium substitution in fish and mouse [Zn_7^{2+}]-MT was measured spectrophotometrically. Cadmium (21 μM) was incubated with fish or mouse MT (2 μM) in 0.2 M Tris-HCl (pH 7.4), and the formation of the Cd-thiolate complex was followed by measuring the absorbance at 254 nm. At the end of the reaction, samples were dialyzed, and the cadmium content was determined by atomic absorption spectroscopy with a Perkin Elmer 5100 PC apparatus equipped with a Zeeman furnace.

Acknowledgments

P.A.T. wishes to thank Prof. Neri Niccolai for constant encouragement and helpful suggestions and Asia Motti for inspiration.

Received: October 31, 2002
Revised: December 20, 2002
Accepted: February 12, 2003
Published: April 1, 2003

References

1. Kägi, J.H.R. (1991). Overview of metallothionein. Methods Enzymol. *205*, 613–626.
2. Templeton, D.M., and Cherian, M.G. (1991). Toxicological significance of metallothionein. Methods Enzymol. *205*, 11–24.
3. Arseniev, A., Schultze, P., Wörgötter, E., Braun, W., Wagner, G., Vašák, M., Kägi, J.H.R., and Wüthrich, K. (1988). Three-dimensional structure of rabbit liver [Cd $_7$]-metallothionein-2a in aqueous solution determined by nuclear magnetic resonance. J. Mol. Biol. *201*, 637–657.
4. Braun, W., Wagner, G., Wörgötter, E., Vašák, M., Kägi, J.H.R., and Wüthrich, K. (1986). Polypeptide fold in the two metal clusters of metallothionein-2 by nuclear magnetic resonance in solution. J. Mol. Biol. *187*, 125–129.
5. Messerle, B.A., Schäffer, A., Vašák, M., Kägi, J.H.R., and Wüthrich, K. (1990). Three-dimensional structure of human [$^{113}Cd_7$]-metallothionein-2 in solution determined by nuclear magnetic resonance spectroscopy. J. Mol. Biol. *214*, 765–779.
6. Narula, S.S., Brouwer, M., Hua, Y., and Armitage, I.M. (1995). Three-dimensional solution structure of Callinectes sapidus metallothionein-I determined by homonuclear and heteronuclear magnetic resonance spectroscopy. Biochemistry *34*, 620–631.
7. Peterson, C.W., Narula, S.S., and Armitage, I.M. (1996). 3D solu-

tion structure of copper- and silver-substituted yeast metallothioneins. FEBS Lett. *379*, 85–93.

8. Riek, R., Prêcheur, B., Wang, Y., Mackay, E.A., Wider, G., Güntert, P., Liu, A., Kägi, J.H.R., and Wüthrich, K. (1999). NMR structure of the sea urchin (Strangylocentrotus purpuratus) metallothionein MTA. J. Mol. Biol. *291*, 417–428.
9. Schultze, P., Wörgötter, E., Braun, W., Wagner, G., Vašák, M., Kägi, J.H.R., and Wüthrich, K. (1988). Conformation of $[Cd_7]$-metallothionem-2 from rat liver in aqueous solution determined by nuclear magnetic resonance spectroscopy. J. Mol. Biol. *203*, 251–268.
10. Robbins, A.H., McRee, D.E., Williamson, M., Collett, S.A., Xuong, N.H., Furey, W.F., Wang, B.C., and Stout, C.D. (1991). Refined crystal structure of Cd, Zn metallothionein at 2.0 Å resolution. J. Mol. Biol. *221*, 1260–1293.
11. Braun, W., Vašák, M., Robbins, A.I.-I., Stout, C.D., Wagner, G., Kägi, J.H.R., and Wüthrich, K. (1992). Comparison of the NMR solution structure and the X-ray crystal structure of rat metallothionein-2. Proc. Natl. Acad. Sci. USA *89*, 10124–10128.
12. Scudiero, R., Carginale, V., Riggio, M., Capasso, C., Capasso, A., Kille, P., di Prisco, G., and Parisi, E. (1997). Difference in hepatic metallothionein content in Antarctic red-blooded and haemoglobinless fish: undetectable metallothionein levels in haemoglobinless fish is accompanied by accumulation of untranslated metallothionein mRNA. Biochem. J. *322*, 207–211.
13. Carginale, V., Scudiero, R., Capasso, C., Capasso, A., Kille, P., di Prisco, G., and Parisi, E. (1998). Cadmium-induced differential accumulation of metallothionein isoforms in the Antarctic icefish, which exhibits no basal metallothionein protein but high endogenous mRNA levels. Biochem. J. *332*, 475–481.
14. Bargelloni, L., Scudiero, R., Parisi, E., Carginale, V., Capasso, C., and Patarnello, T. (1999). Metallothioneins in antarctic fish: evidence for independent duplication and gene conversion. Mol. Biol. Evol. *16*, 885–897.
15. D'Auria, S., Carginale, V., Scudiero, R., Crescenzi, O., Di Maro, D., Temussi, P.A., Parisi, E., and Capasso, C. (2001). Structural characterisation and thermal stability of Notothenia coriiceps metallothionein. Biochem. J. *354*, 291–299.
16. Aue, W.P., Bartholdi, E., and Ernst, R.R. (1976). Two-dimensional spectroscopy. Application to nuclear magnetic resonance. J. Chem. Phys. *64*, 2229–2246.
17. Bax, A., and Davis, D.G. (1985). MLEV-17 based two-dimensional homonuclear magnetization transfer spectroscopy. J. Magn. Reson. *65*, 355–360.
18. Jeener, J., Meier, B.H., Bachmann, P., and Ernst, R.R. (1979). Investigation of exchange processes by two-dimensional NMR spectroscopy. J. Chem. Phys. *71*, 4546–4553.
19. Güntert, P., Braun, W., Billeter, M., and Wüthrich, K. (1989). Automated stereospecific 1H NMR assignments and their impact on the precision of protein structure determinations in solution. J. Am. Chem. Soc. *111*, 3997–4004.
20. Frey, M.H., Wagner, G., Vasak, M., Sorensen, O.W., Neuhaus, D., Worgotter, E., Kagi, J.H.R., Ernst, R.R., and Wuthrich, K. (1985). Polypeptide-metal cluster connectivities in metallothionein-2 by novel ^{1}H ^{113}Cd heteronuclear two-dimensional NMR experiments. J. Am. Chem. Soc. *107*, 6847–6851.
21. Johnson, B.A., and Blevins, R.A. (1994). NMRView: a computer program for the visualization and analysis of NMR data (1994). J. Biomol. NMR *4*, 603–614.
22. Güntert, P., Mumenthaler, C., and Wüthrich, K. (1997). Torsion angle dynamics for NMR structure calculation with the new program DYANA. J. Mol. Biol. *273*, 283–298.
23. Güntert, P., Braun, W., and Wüthrich, K. (1991). Efficient computation of three-dimensional protein structures in solution from nuclear magnetic resonance data using the program DIANA and the supporting programs CALIBA, HABAS and GLOMSA. J. Mol. Biol. *217*, 517–530.
24. Kim, Y., and Prestegard, J.H. (1989). Measurement of vicinal couplings from cross peaks in COSY spectra. J. Magn. Reson. *84*, 9–13.
25. Titman, J.J., and Keeler, J.A. (1990). Measurement of homonuclear coupling constants from NMR correlation spectra. J. Magn. Reson. *89*, 640–646.
26. Griesinger, C., Soerensen, O.W., and Ernst, R.R. (1985). Two dimensional correlation of connected NMR transitions. J. Am. Chem. Soc. *107*, 6394–6396.
27. Pearlman, D.A., Case, D.A., Caldwell, J.W., Ross, W.S., Cheatham, T.E., III, DeBolt, S., Ferguson, D., Seibel, G., and Kollman, P.A. (1995). AMBER, a computer program for applying molecular mechanics, normal mode analysis, molecular dynamics and free energy calculations to elucidate the structures and energies of molecules. Comput. Phys. Commun. *91*, 1–41.
28. Zangger, K., and Armitage, I.M. (2002). Dynamics of interdomain and intermolecular interactions in mammalian metallothioneins. J. Inorg. Biochem. *88*, 135–143.
29. Pan, P.K., Hou, F., Cody, C.W., and Huang, P.C. (1994). Substitution of glutamic acids for the conserved lysines in the α-domain affects metal-binding in both the α- and β-domains of mammalian metallothionein. Biochem. Biophys. Res. Commun. *202*, 621–628.
30. Kay, J., Cryer, A., Darke, B.M., Kille, P., Lees, W.E., Norey, C.G., and Stark, J.M. (1991). Naturally occurring and recombinant metallothioneins: structure, immunoreactivity and metal-binding functions. Int. J. Biochem. *23*, 1–5.
31. Dallinger, R., Berger, B., Hunziker, P., and Kagi, J.H.R. (1997). Metallothionein in snail Cd and Cu metabolism. Nature *388*, 237–238.
32. Zangger, K., Oz, G., Otvos, J.D., and Armitage, I.M. (1999). Three-dimensional solution structure of mouse [Cd7]-metallothionein-1 by homonuclear and heteronuclear NMR spectroscopy. Protein Sci. *8*, 2630–2638.
33. Xiong, Y., and Ru, B. (1997). Purification and characteristics of recombinant mouse metallothionein-I from Escherichia coli. J. Biochem. (Tokyo) *121*, 1102–1106.
34. Capasso, C., Abugo, O., Tanfani, F., Scire, A., Carginale, V., Scudiero, R., Parisi, E., and D'Auria, S. (2002). Stability and conformational dynamics of metallothioneins from the antarctic fish Notothenia coriiceps and mouse. Proteins *46*, 259–267.
35. Delaglio, F., Grzesiek, S., Vuister, G.W., Zhu, G., Pfeifer, J., and Bax, A. (1995). NMRpipe—a multidimensional spectral processing system based on unix PIPES. J. Biomol. NMR *6*, 277–293.
36. Mareci, T.H., and Freeman, R. (1983). Mapping proton-proton coupling via double quantum coherence. J. Magn. Reson. *51*, 531–535.
37. Wüthrich, K. (1986). NMR of proteins and nucleic acids (New York: John Wiley and Sons).
38. Cavanagh, J., and Rance, M. (1992). Suppression of cross-relaxation effects in TOCSY spectra via a modified DIPSI-2 mixing sequence. J. Magn. Reson. *96*, 670–678.
39. Marion, D., and Wüthrich, K. (1983). Application of phase sensitive two dimensional correlated spectroscopy (COSY) for measurements of H-H spin-spin coupling constants in proteins. Biochem. Biophys. Res. Commun. *113*, 967–974.
40. Piotto, M., Saudek, V., and Sklenar, V. (1992). Gradient-tailored excitation for single-quantum NMR spectroscopy of aqueous solutions. J. Biomol. NMR *2*, 661–665.
41. Koradi, R., Billeter, M., and Wüthrich, K. (1996). MOLMOL: a program for display and analysis of macromolecular structures. J. Mol. Graph. *14*, 51–55.
42. Capasso, C., Carginale, V., Scudiero, R., Crescenzi, O., Spadaccini, R., Temussi, P.A., and Parisi, E. (2003). Phylogenetic divergence of fish and mammalian metallothionein. Relationships with structural diversification and organismal temperature. J. Mol. Evol., in press.
43. Jiang, L.J., Vasak, M., Vallee, B.L., and Maret, W. (2000). Zinc transfer potentials of the α- and β-clusters of metallothionein are affected by domain interactions in the whole molecule. Proc. Natl. Acad. Sci. USA *97*, 2503–2508.
44. Thompson, J.D., Gibson, T.J., Plewniak, F., Jeanmougin, F., and Higgins, D.G. (1997). The CLUSTAL_X windows interface: flexible strategies for multiple sequence alignment aided by quality analysis tools. Nucleic Acids Res. *24*, 4876–4882.

Accession Numbers

The coordinates and restraints of MT_nc were deposited into the Protein Data Bank. The accession codes for the coordinate data of the α and β domains are 1M0G and 1M0J, respectively.